Available online at www.sciencedirect.com
SCIENCE DIRECT®
Journal of Nuclear Materials 337–339 (2005) 271–275
journal of nuclear materials
www.elsevier.com/locate/jnucmat

EDGE2D code simulations of SOL flows and in–out divertor asymmetries in JET

G.S. Kirnev [a,*], G. Corrigan [b], D. Coster [c], S.K. Erents [b], W. Fundamenski [b], G.F. Matthews [b], R.A. Pitts [d]

[a] *Nuclear Fusion Institute, RRC 'Kurchatov Institute', Kurchatov sq. 1, Moscow 123182, Russia*
[b] *Euratom/UKAEA Fusion Association, Culham Science Centre, Abingdon, Oxfordshire, OX14 3DB, UK*
[c] *Max-Planck-Institut für Plasmaphysik, Association Euratom-IPP, Garching, Germany*
[d] *Centre de Recherches en Physique des Plasmas, Association Euratom-Confédération Suisse, Ecole Polytechnique Fédérale de Lausanne, CH-1015 Lausanne, Switzerland*

Abstract

EDGE2D simulations show that high SOL flows can be generated when an additional radial convective transport is applied in the SOL and pedestal region along with a 'ballooning-like' poloidal variation in transport. This model produces an inward particle flux at the inboard side of the plasma along with an enhanced outward flux at the outer midplane. Parallel Mach numbers can be produced at the top of the machine which are comparable in magnitude to those observed by the JET Mach probes. For the normal toroidal magnetic field direction, the parallel flow Mach number is about $M = 0.32$ in this case. Applying these two additional mechanisms also allows experimental outer to inner target power and out–in divertor line emission intensity asymmetries to be qualitatively reproduced.

PACS: 52.25.Fi; 52.55.Fa; 55.65.Kj
Keywords: 2D modelling; Parallel particle flow; Divertor asymmetry; JET

1. Introduction

The mechanisms underlying the generation of parallel plasma flow play a significant role in our understanding of transport physics [1]. In particular, plasma flows are important contributors to plasma recycling and impurity transport in the scrape-off layer (SOL) [2] and in–out divertor target power and particle asymmetries [1,3–5]. Understanding these flow drive mechanisms is therefore central to explaining the observed asymmetries in particle and power flux in the divertor and in impurity pumping and redeposition.

In JET, a high velocity parallel flow (Mach number $M = 0.4$–0.6) is observed by a Mach probe located near the top, low field side (LFS) of the machine when the ion grad B drift is directed downwards, towards the lower X-point (normal field direction) [6]. When the direction of the magnetic field, B_T and plasma current, I_p are reversed, the measured flow across most of the SOL, falls to a low value, typically $-0.1 < M < 0.1$. Previous code simulations [7], with the 2D multi-fluid code

* Corresponding author. Tel.: +7 095 1967808; fax: +7 095 9430073.
E-mail address: kirnev@fusion.ru (G.S. Kirnev).

0022-3115/$ - see front matter © 2004 Elsevier B.V. All rights reserved.
doi:10.1016/j.jnucmat.2004.09.032

EDGE2D/NIMBUS [8,9] have satisfactorily reproduced the general shape of $M(r)$ and the target asymmetry measured in JET field reversal experiments. However, in normal field discharges, the measured parallel Mach number is a factor 3–5 higher than that predicted by EDGE2D [6]. This discrepancy is not unique to EDGE2D simulations with classical drifts since similar results have been obtained for JET [10,11] when using both the UEDGE [12] and SOLPS5.0 [13,14] codes. So, whilst qualitatively consistent with experiment in general form and dependence on the sign of the magnetic field, the absolute value of the flow measured at this specific poloidal location in JET, appears to present a problem for all code packages that have been tried. Fast parallel SOL flows towards the inner divertor at the high-field-side (HFS) SOL have been measured in both C-Mod [15] and JT-60U [16]. When applied to the latter results, the UEDGE code with drift terms switched on reproduces qualitatively the poloidal distribution of parallel flow but not the magnitude [17].

This quantitative disagreement in measured and simulated parallel Mach numbers suggests further that mechanisms other than classical drifts might be driving the SOL flow (or of course that the drift terms are incorrectly included in the codes!). Several attempts have been made to explain the high JET flows including the adhoc addition of external momentum sources in the SOL [18] and carbon impurities generated at the probe by plasma–surface interaction [6]. In this paper we consider two additional mechanisms. First, a major finding of the experimental measurements is that the radial flow profile, $M(r)$, is not symmetric around the zero axis when the field is reversed, but instead around an offset value of $M \sim 0.2$. It has been suggested that this might be caused by an additional, field independent mechanism, such as 'ballooning' type radial transport which generates a larger efflux of particles from the core into the SOL at the outer mid-plane. In JET, the experimentally measured total turbulent particle flux, $\Gamma_\perp$, is about $1\text{–}2 \times 10^{20}\ \mathrm{m^{-2}\,s^{-1}}$ at the separatrix at LFS [19]. According to results obtained from other tokamaks [20–23] we assume the turbulent flux at the high field side (HFS) to be about two times lower than at the LFS. In the present modelling we describe the total turbulent flux by an effective diffusion coefficient, $D_\perp$, with an inverse dependence on B_T.

It is obvious that the turbulent flux must be field independent and therefore cannot be responsible for the parallel flow asymmetry seen when inverting the direction of B_T. We suppose that a second transport process, an additional radial, quasi-stationary convection, provides mechanism by which the total particle flux maybe increased or decreased depending on the direction of B_T. To modify the total particle flux this convective component should be of the same order as the turbulent contribution. Assuming a convective flux magnitude of $10^{20}\ \mathrm{m^{-2}\,s^{-1}}$, a radial velocity up to $10\ \mathrm{ms^{-1}}$ is possible if the plasma density is $10^{19}\ \mathrm{m^{-3}}$. In the modelling, we specify the quasi-stationary convection as an input parameter – the pinch velocity V_{pinch}. For the case of normal B_T direction, an outward convective flux at the LFS and an inward flux at the HFS are imposed. This is assumed to result in an increase of the in–out SOL pressure asymmetry and a corresponding parallel flow from the outboard to inboard side. In reversed field, the adhoc convective flux direction is reversed giving an inward flux at the LFS and an outward (i.e. directed to the HFS) flux at the HFS leading to a decrease in the in–out pressure asymmetry.

We do not pretend here to be able to propose the origin of the underlying mechanism that drives the convective plasma motion. One such mechanism leading to the convective flux in the SOL can be a radial drift in the poloidal electric field E_θ [5,24,25]. However, the 2D fluid code calculates a value of E_θ that would be too low by a factor of $\sim$10 to generate the proposed radial flux velocity of 10 m/s.

Despite the ad-hoc nature of this approach, the following section will show that the inclusion of an additional convective transport mechanism allows us to reproduce a number of the experimentally observed trends that cannot be matched by the code when classical drift terms alone are included.

2. Results of modelling

To study the influence of the additional transport on the SOL and divertor parameters a regime with fixed separatrix density $0.8 \times 10^{19}\ \mathrm{m^{-3}}$ has been chosen. This is a relatively low density in which drift flows might be expected to be relatively high. Power entering the SOL is varied in the range 1–4.5 MW with deuterium the main plasma species. Ion and electron heat conductivities, χ_i, χ_e, and $D_\perp$ are all fixed to a value of $0.5\ \mathrm{m^2\,s^{-1}}$ at the outer midplane separatrix. Due to the assumed inverse dependence of the transport coefficients on B_T, $D_\perp$ is lower by about a factor 1.8 at the inner midplane. An additional flux expansion dependence of the transport (due to the Shafranov shift) has not been taken into account (this would lead to a LFS/HFS midplane $D_\perp$ ratio of $\sim$1.4). Throughout the SOL and into the pedestal region (about 2 cm inside the separatrix) $V_{\mathrm{pinch}} = 10\ \mathrm{ms^{-1}}$ is imposed. Carbon impurity was included in all calculations to which the same assumptions regarding transport coefficients and V_{pinch} are applied. At the inner an outer boundaries of the simulation grid, a boundary condition of $V_{||} = 0$ are imposed. With the exception of some cases to be discussed later, all drifts were switched off in the simulations.

Fig. 1 presents radial profiles of $\Gamma_\perp$ for both field directions at the outer and inner midplanes. The value

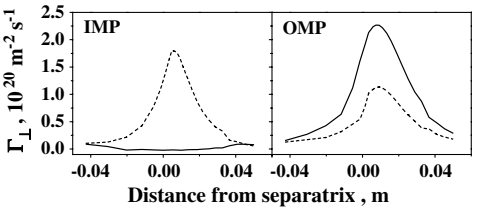

Fig. 1. Radial profiles of the total perpendicular particle flux at outer (OMP) and inner midplanes (IMP) for normal (——) and reversed (---) B_T cases. P_{SOL} = 2.5 MW.

of the outboard particle flux $\Gamma_\perp$ is about $2 \times 10^{20}\,m^{-2}\,s^{-1}$ in the normal field case. This value is halved when the outboard radial convection is reversed (reversed field case). At the HFS, convective transport is comparable to the turbulent component, leading to a very low total particle flux in the normal field case since the radial convection is inward. In reversed field the additional outward convection leads to an increase of the total particle flux at the HFS so that it becomes comparable with the outboard total flux. Such a particle flux would be expected to result in modification of the plasma pressure. It should be noted that the radial profiles of the density are slightly different for normal and reverse field cases.

Poloidal profiles of the total (ion and electron) static pressure calculated at a radius r_{sep} + 1.5 cm (with r_{sep} is the separatrix radius) are shown in Fig. 2. A large parallel gradient directed from the inboard to outboard sides is clearly apparent in the normal field case and would be expected to generate particle flow to the HFS. In reversed field, the HFS directed convective flux decreases the outboard plasma pressure and the parallel pressure gradient disappears.

Fig. 3 compiles a number of simulated Mach number profiles at the poloidal position corresponding to the Mach probe location. In the convention adopted here, positive M corresponds to a flow directed towards the inner divertor. The parallel flows clearly differ strongly for the two different magnetic field directions (curves 1

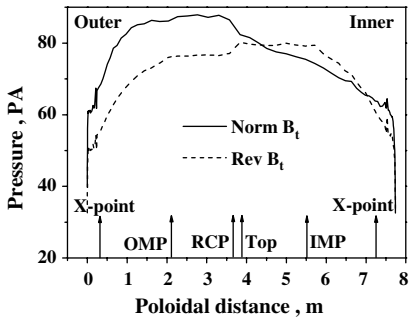

Fig. 2. Poloidal profiles of the total static pressure for both field directions (RCP – Mach probe location). P_{SOL} = 2.5 MW.

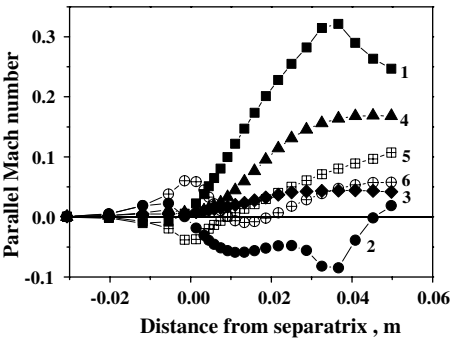

Fig. 3. Radial profiles of the parallel Mach number at the JET Mach probe location for different cases. 1, 2: with radial convection for normal and reversed B_T directions; 3: without radial convection and poloidally constant $D_\perp$; 4: without pinch and with poloidal dependence of $D_\perp$; 5, 6: cases with all classical drifts switched on and poloidally constant $D_\perp$ for normal and reversed B_T directions. P_{SOL} = 2.5 MW.

and 2). For reversed field (curve 2) the Mach number $M \sim 0$ everywhere in the SOL. In contrast, M increases with radius in the normal field case (curve 1) reaching a value of $M \approx 0.32$ at a distance of r_{sep} = 3–4 cm. This is not far from the experimentally measured values.

For comparison, Fig. 3 also includes simulated M profiles computed in the absence of the additional radial convection. Curves 3 and 4 were respectively obtained without and with the assumption of poloidally dependent transport coefficients. When the radial transport is assumed independent of the magnitude of B_T, $M < 0.1$. The ballooning-like transport leads to an increase of the in–out plasma pressure asymmetry and the parallel flow toward the inner divertor rises. However, this effect on its own does not seem to lead to parallel Mach numbers greater than 0.17, which remain low in comparison with experimental measurements. They are nevertheless still in excess of what is predicted when only classical drifts (ΔB, $E \times B$ and centrifugal on both D and C ions) are applied (curves 5 and 6 in Fig. 3). In these latter cases, transport coefficients were maintained constant in the poloidal direction and drifts were switched on only in the SOL. (though similar results have been obtained in [6] with both core and SOL drifts switched on). The difference between the normal and reversed field cases is insignificant for the conditions and input parameters chosen for the simulation. However, as also found in [6], the difference in $M(r)$ at the probe location between the two field directions is dependent on the separatrix plasma density and increases with density for both normal and reversed B_T. It should also be emphasized that the calculated poloidal electric field is very low, about 0.02 V/cm, and is thus several times lower than that which would be required to generate a radial convective flux with a velocity $V_{pinch} = 10\ ms^{-1}$.

As mentioned above, the arithmetic mean between the normal and reversed field measurements of M is about 0.2 across the SOL. The calculated value of M is very close to the experimental value in the 'far' SOL in case of poloidal variation of the transport coefficients (Fig. 3, curve 4). However, in all cases the parallel Mach number decreases in the vicinity of the separatrix and does not therefore match the experiment.

We now consider the influence of radial convection on asymmetry of the divertor plasma parameters using the examples of simulated cases 1 and 2 in Fig. 3. From experiment we know that strong out–in target power and particle asymmetries exist in JET [26]. Fig. 4 presents the simulated and experimental dependencies of the target power asymmetry, $A_{\mathrm{out/in}}$, on P_{SOL}, the power entering the SOL. In the experiment, P_{SOL} is computed as the total heating power minus radiated power in the plasma core. The experimental values of $A_{\mathrm{out/in}}$ are derived from divertor thermocouple measurements of the inner and outer vertical tile temperatures in L-mode discharges (strike points are positioned on these tiles). For comparison, the simulated values are computed as the ratio of outer to inner total power loads integrated over the target plates. For $P_{\mathrm{SOL}} < 3$ MW, the experimental ratios are linearly dependent on P_{SOL}, saturating somewhat at higher values of input power into the SOL. For normal field, the simulated asymmetry increases linearly with power P_{SOL} and therefore slightly exceeds the experimental values at the highest P_{SOL}. In reversed field, simulation is entirely consistent the experiment.

Comparison of the results of simulations with experimental values for the out–in divertor asymmetry of the D_α and CIII line emission intensities has also been performed and the results summarized in Fig. 5. Experimental D_α and CIII emission asymmetries depend only slightly on P_{SOL} in reversed magnetic field. In normal field, the D_α out–in asymmetry decreases and the CIII asymmetry increases with input power, especially for $P_{\mathrm{SOL}} > 2$ MW. Both the experimental and simulated emission intensities are integral values, including, for each divertor the total volume covered by the spectroscopic lines of sight. Fig. 5 demonstrates that the calculated results are in qualitative agreement with the experimental data. We note that in all simulations of divertor asymmetry all input parameters other than the power entering the SOL have been held constant.

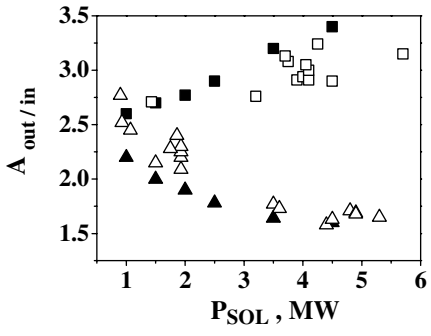

Fig. 4. Experimental and simulated target power asymmetries versus power entering to the SOL. ■ – EDGE2D, normal field; ▲ – EDGE2D, reversed field; □ – experiment, normal field; △ – experiment, reversed field.

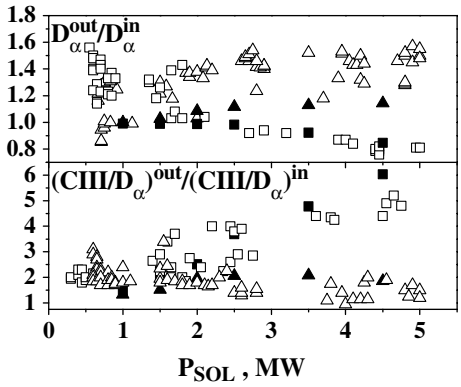

Fig. 5. Out–in D_α and CIII divertor emission intensity asymmetry versus power entering to the SOL. ■ – EDGE2D, normal field; ▲ – EDGE2D, reversed field; □ – experiment, normal field; △ – experiment, reversed field. Note that the CIII intensities are normalised to the D_α intensity to provide an approximate measure of the impurity production rate.

3. Conclusions

Simulations with the EDGE2D/NIMBUS code show that an additional field independent mechanism such as 'ballooning' generating a larger efflux of particles from the core into the SOL at the outer midplane can lead to an increase of the in–out plasma pressure and as a consequence to an increased parallel flow towards the inner divertor. This effect on its own, however, cannot produce parallel Mach numbers in excess of ~0.17 in our simulations and is still considerably lower the than experimentally measured values.

By including an additional radial convection along with a 'ballooning-like' poloidal variation in transport, stronger SOL flows can be generated. Parallel Mach numbers can be produced at the top, low field side of the machine which are comparable with the magnitude of those observed by the JET Mach probes. The maximum simulated normal field parallel Mach number is about $M = 0.32$ without switching on classical drift terms.

Applying these two additional mechanisms also allows the experimental trends with power entering the SOL of the outer to inner target power asymmetry and

out–in divertor D_α and CIII emission intensity asymmetries to be reproduced without varying the assumptions.

We are not aware of a physical basis for the radial convective plasma transport proposed here. Nevertheless, the inclusion of such a mechanism into the code allows us to reproduce some of the experimentally observed trends without recourse to a case by case adjustment of the assumptions. For as long as anomalous cross-field transport is poorly understood and codes including classical drifts effects fail to quantitatively match experimental data, the possibility that convection effects contribute to SOL flow should remain open.

Acknowledgments

This work is supported by Bilateral Agreement between the European Atomic Energy Community and the Government of the Russian Federation in the field of Controlled Nuclear Fusion. The work was also supported by INTAS-01-0457.

References

[1] A.V. Chankin, P.C. Stangeby, Plasma Phys. Control. Fusion 36 (1994) 1485.
[2] M. Keilhacker et al., Plasma physics and controlled nuclear fusion research IAEA 1990 Report IAEA-CN-53/A-V-1.
[3] R.H. Cohen, D.D. Ryutov, Comment. Plasma Phys. Control. Fus. 16 (1995) 255.
[4] M. Tendler, V. Rozhansky, Comment. Plasma Phys. Control. Fus. 13 (1990) 191.
[5] P.C. Stangeby, A.V. Chankin, Nucl. Fus. 36 (1996) 839.
[6] S.K. Erents et al., Plasma Phys. Control. Fus. 46 (2004) 1757.
[7] A.V. Chankin et al., J. Nucl. Mater. 290–293 (2001) 518.
[8] G.J. Radford, A.V. Chankin, G. Corrigan, et al., Contrib. Plasma Phys. 36 (1996) 187.
[9] A.V. Chankin, J.P. Coad, G. Corrigan, et al., Contrib. Plasma Phys. 40 (2000) 288.
[10] G.D. Porter et al., J. Nucl. Mater. 313–316 (2003) 1085.
[11] D. Coster et al., these Proceedings. doi:10.1016/j.jnucmat.2004.10.013.
[12] T.D. Rognlien, D.D. Ryutov, Contrib. Plasma Phys. 38 (1998) 152.
[13] R. Schneider et al., J. Nucl. Mater. 266–269 (1999) 175.
[14] V. Rozhansky et al., Nucl. Fus. 41 (2001) 387.
[15] B. LaBombard et al., in: Proceedings of the 16th International Conference on the Plasma Surface Interactions in Controlled Fusion Devices, Portland Maine, USA, 24–28 May 2004.
[16] N. Asakura et al., Plasma Phys. Control. Fus. 44 (2002) 2101.
[17] N. Asakura et al., Nucl. Fus. 44 (2004) 503.
[18] J.D. Strachan et al., these Proceedings. doi:10.1016/j.jnucmat.2004.09.069.
[19] C. Hidalgo et al., Plasma Phys. Control. Fus. 44 (2002) 1557.
[20] B. LaBombard, B. Lipschultz, Nucl. Fus. 27 (1987) 81.
[21] M. Endler et al., Nucl. Fus. 35 (1995) 1307.
[22] V.A. Vershkov et al., J. Nucl. Mater. 241–243 (1997) 873.
[23] J.L. Terry et al., Phys. Plasmas 10 (2003) 1739.
[24] A.V. Nedospasov et al., Nucl. Fus. 26 (1986) 1529.
[25] V.G. Petrov, Nucl. Fus. 24 (1984) 259.
[26] R.A. Pitts et al., these Proceedings. doi:10.1016/j.jnucmat.2004.10.111.